AD-A040 318   VERMONT UNIV BURLINGTON DEPT OF CHEMISTRY   F/G 7/2
                MOSSBAUER AND MAGNETIC STUDIES OF A MIXED-VALENCE FERRIMAGNET, --ETC(U)
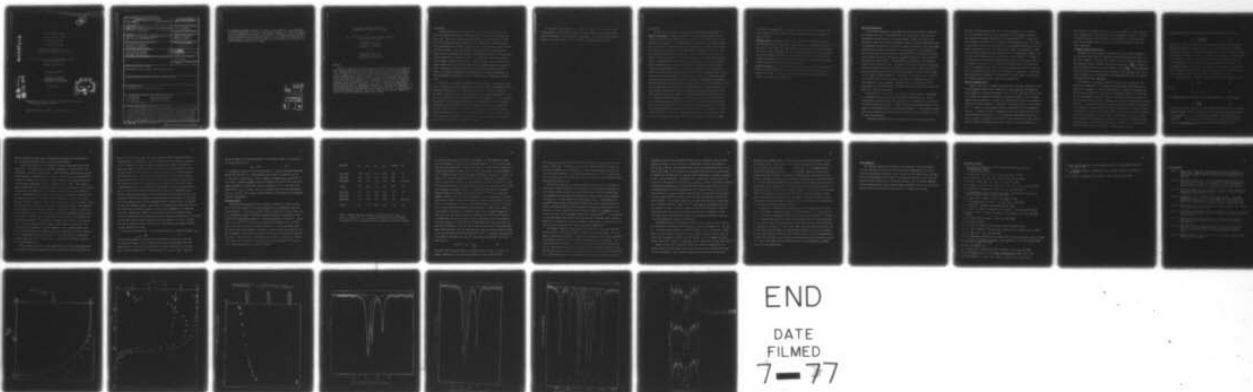   MAY 77   E G WALTON, D B BROWN, H WONG   N00014-75-C-0756
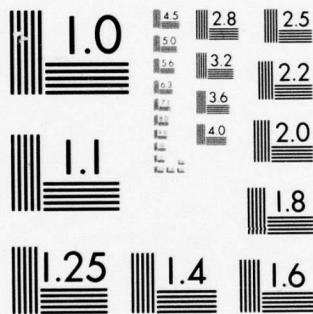UNCLASSIFIED   TR-6   NL

| OF |
AD
A040318

END
DATE
FILMED
7—77

MICROCOPY RESOLUTION TEST CHART

NATIONAL BUREAU OF STANDARDS-1963-A

MÖSSBAUER AND MAGNETIC STUDIES OF A
MIXED-VALENCE FERRIMAGNET, $Fe_2F_5 \cdot 2H_2O$

by

Erick G. Walton, David B. Brown, Herbert Wong and
William Michael Reiff

Prepared for Publication

in

Inorganic Chemistry

University of Vermont
Department of Chemistry
Burlington, Vermont 05401

May 6, 1977

REPORT DOCUMENTATION PAGE		READ INSTRUCTIONS BEFORE COMPLETING FORM
1. REPORT NUMBER TR-6	2. GOVT ACCESSION NO.	3. RECIPIENT'S CATALOG NUMBER
4. TITLE (and Subtitle) MOSSBAUER AND MAGNETIC STUDIES OF A MIXED-VALENCE FERRIMAGNET, $Fe_2F_5 \cdot 2H_2O$		5. TYPE OF REPORT & PERIOD COVERED Technical Report
		6. PERFORMING ORG. REPORT NUMBER
7. AUTHOR(s) E.G. Walton, D.B. Brown, H. Wong (Northeastern U.) and W.M. Reiff (Northeastern U.)		8. CONTRACT OR GRANT NUMBER(s) N00014-75-C-0756
9. PERFORMING ORGANIZATION NAME AND ADDRESS Department of Chemistry University of Vermont Burlington, Vermont 05401		10. PROGRAM ELEMENT, PROJECT, TASK AREA & WORK UNIT NUMBERS
11. CONTROLLING OFFICE NAME AND ADDRESS Office of Naval Research Department of the Navy Arlington, Virginia 22217		12. REPORT DATE May 1977
		13. NUMBER OF PAGES 32
14. MONITORING AGENCY NAME & ADDRESS(if different from Controlling Office)		15. SECURITY CLASS. (of this report) Unclassified
		15a. DECLASSIFICATION/DOWNGRADING SCHEDULE

16. DISTRIBUTION STATEMENT (of this Report)

Approved for Public Release, Distribution Unlimited

17. DISTRIBUTION STATEMENT (of the abstract entered in Block 20, if different from Report)

18. SUPPLEMENTARY NOTES

To be published in Inorganic Chemistry

19. KEY WORDS (Continue on reverse side if necessary and identify by block number)

Iron Complexes	Spontaneous magnetization
Mixed-Valence	Hyperfine Interactions
Ferrimagnetism	Molecular Field Theory
Mossbauer Spectroscopy	

20. ABSTRACT (Continue on reverse side if necessary and identify by block number)

The red, crystalline mixed-valence compound pentafluorodiiron(II,III)dihydrate, $Fe_2F_5 \cdot 2H_2O$, has been examined using Mössbauer spectroscopy and magnetic susceptibilities. At 48K the material orders ferrimagnetically as the result of spin compensation of iron(III) by iron(II). Above this critical temperature, the observation of distinct quadrupole-split Mössbauer absorptions for iron(II) and iron(III) sites demonstrates the non-equivalence of oxidation states and establishes $Fe_2F_5 \cdot 2H_2O$ as a Class II mixed-valence compound. In the temperature range 49-380 K, the magnetic susceptibility may

DD $_{1 JAN 73}^{FORM}$ 1473 EDITION OF 1 NOV 65 IS OBSOLETE

be explained using the molecular field theory of ferrimagnetism. Long range order is observed below 48K. This order is demonstrated magnetically through the observation of spontaneous magnetization, field-dependent susceptibilities, and a saturation moment corresponding to a formula unit spin of $S = \frac{1}{2}$. Mossbauer spectra below the critical temperature exhibit magnetic hyperfine structure consistent with the ferrimagnetic ordering. Hysteresis in the magnetic behavior suggests the possibility of a low-temperature magnetic phase change.

Mössbauer and Magnetic Studies of a
Mixed-Valence Ferrimagnet, $Fe_2F_5 \cdot 2H_2O$

by

Erick G. Walton,[1a] David B. Brown,[1b*] Herbert Wong,[1c]
and William Michael Reiff[1c]

Department of Chemistry
University of Vermont
Burlington, Vermont 05401

and

Department of Chemistry
Northeastern University
Boston, Massachusetts 02115

Abstract

The red, crystalline mixed-valence compound pentafluorodiiron(II,III)dihydrate,
$Fe_2F_5 \cdot 2H_2O$, has been examined using Mössbauer spectroscopy and magnetic susceptibili-
ties. At 48K the material orders ferrimagnetically as the result of spin compensa-
tion of iron(III) by iron(II). Above this critical temperature, the observation of
distinct quadrupole-split Mössbauer absorptions for iron(II) and iron(III) sites
demonstrates the non-equivalence of oxidation states and establishes $Fe_2F_5 \cdot 2H_2O$ as
a Class II mixed-valence compound. In the temperature range 49-300 K, the magnetic
susceptibility may be explained using the molecular field theory of ferrimagnetism.
Long range order is observed below 48K. This order is demonstrated magnetically
through the observation of spontaneous magnetization, field-dependent susceptibilities,
and a saturation moment corresponding to a formula unit spin of $S = \frac{1}{2}$. Mössbauer
spectra below the critical temperature exhibit magnetic hyperfine structure consistent
with the ferrimagnetic ordering. Hysteresis in the magnetic behavior suggests the
possibility of a low-temperature magnetic phase change.

Introduction

In 1958 Brauer and Eichner[2] reported that the interaction of metallic iron with hot concentrated hydrofluoric acid gave rise to a yellow solid of composition $Fe_2F_5 \cdot 7H_2O$. They further showed that this material could be dehydrated, at 100°C, to a red trihydrate and that at 180°C reversible dehydration to a blue-grey anhydrous mixed-valence iron fluoride, Fe_2F_5, occurred. This system has aroused interest for several reasons. First, the variety of colors exhibited by these materials suggests that the complexes span a range of mixed-valence behavior,[3] and thus provide a unique opportunity to examine variations in mixed-valence interactions with only minimal changes in empirical formulation. Second, the fluoride ion is known to be a unique species which is particularly effective as a bridging ligand with transition metals, suggesting at least the possibility of long range cooperative effects.[4] Finally, the systems are amenable to investigation by a variety of techniques, including Mössbauer spectroscopy and the field and temperature dependence of magnetization.

Through the use of magnetic susceptibilities and Mössbauer spectroscopy we have recently formulated the yellow heptahydrate as the ionic Class I mixed-valence species $[Fe(H_2O)_6^{+2}][FeF_5(H_2O)^{-2}]$.[5] A similar conclusion has been reached by Sakai and Tominaga[6] on the basis of X-ray powder patterns and ^{19}F broad-line nmr spectra. The red species described by Brauer and Eichner[2] as the trihydrate is in fact a dihydrate, $Fe_2F_5 \cdot 2H_2O$.[7-9] There has been relatively little characterization of this dihydrate, although Sakai and Tominaga[10] have reported Mössbauer spectra at room temperature and 80°K. While our work was in progress, a more detailed examination of the low temperature Mössbauer spectra of this complex appeared.[11] For the most part, both of these studies are in agreement with our results, and where appropriate, a comparison to these reports will be included in this paper.

On the basis of color alone, the dihydrate is expected to be a Class II mixed-valence complex. In this paper we report the results of our studies, using several physical techniques, on this red complex, $Fe_2F_5 \cdot 2H_2O$. The structure of this material, determined by single crystal X-ray diffraction, has recently been reported.[12]

Experimental

The preparation of crystalline $Fe_2F_5 \cdot 2H_2O$ has been described previously.[12]

Magnetic Measurements: Magnetic susceptibilities were measured independently at the University of Vermont and Northeastern University by the Faraday method, using $HgCo(NCS)_4$ as calibrant.[13] The variable temperature magnetic susceptibility measurements carried out at Northeastern University were made on a Faraday balance composed of a Cahn RG electrobalance, a Varian model 4000 electromagnet with four inch constant force pole caps and a Janis Super Vari-temp. cryostat over the range 1.5 to 300 K for ten fields between 1.6 and 5 kG using quartz fiber suspensions and sample holders. Temperature measurement and control was typically of the order ± 0.01K or better and was achieved using a Leeds-Northrup K-5 potentiometer and a Lake Shore Cryotronics model DT-500C set point controller respectively in conjunction with a calibrated silicon dioxide temperature sensor diode, a ten micro-amp constant current source and an uncalibrated gallium arsenide control diode. Final temperature equilibration and stability were continuously monitored on a Leeds-Northrup Speedomax-XL 600 millivolt recorder that was used to read the error signal of the calibrated silicon dioxide diode after cancellation by the K-5 potentiometer. Temperatures below 4.2 K were measured via the vapor pressure of helium using Wallace-Tiernan models FA-160 and 61-050 absolute pressure gauges while pumping was precisely controlled with an L.J. Engineering model 329 vacuum regulator valve. Temperatures below 78 K and to as low as 50 K were also achieved using liquid nitrogen by pumping (Welch 1397) to well below the triple point on solid nitrogen. Both the vapor pressure of nitrogen and a calibrated silicon dioxide diode were used to monitor the temperature in the region 49 to 78 K. An F.W. Bell model 610 Gaussmeter with a transverse Hall probe was used for measurement of magnetic fields. Data obtained by the Faraday method

were checked, and magnetization measurements from 0 to 45 kG were obtained, using the PAR Models 150 and 151 vibrating sample magnetometers at the University of North Carolina.

Mössbauer Spectra: Mossbauer spectra in the interval 20 - 295°K were obtained as previously described for $Fe_2F_5 \cdot 7H_2O$.[5] Measurements at lower temperatures were obtained with a Janis Super Vari-Temp Cryostat with calibrated silicon dioxide sensor and control diodes. Mössbauer spectra in external (longitudinal) fields were determined at the Francis Bitter National Magnet Laboratory using a Niobium-tin superconducting solenoid in conjunction with a conventional constant acceleration spectrometer and a source of 100 mC ^{57}Co on Rhodium metal.

Electronic Spectra: Diffuse reflectance spectra were recorded at the University of Oxford on a Unicam SP700 double beam spectrophotometer with a Unicam diffuse reflectance attachment. Samples were finely ground and the spectra measured with respect to a magnesium oxide standard.

Results and Discussion

In the yellow heptahydrate, $Fe_2F_5 \cdot 7H_2O$, there are twelve potential ligands for the two metal ions, and in consequence both iron (II) and iron (III) attain six-corrdination with no necessity for bridging ligands. However, the loss of five molecules of water upon forming the dihydrate suggests coordinative unsaturation and, in consequence, the necessity for extensive bridging interactions. This has now been confirmed by the single-crystal X-ray structure determination reported recently.[12] The structure consists of vertex-sharing octahedra $Fe^{III}F_6$ forming parallel zig-zag chains, which in turn are cross-linked by trans-$Fe^{II}F_4(H_2O)_2$ with vertex sharing in the equatorial fluorine plane. Bridging fluorine is suggested by the electronic spectrum of this material as well. The diffuse reflectance spectrum[14] of $Fe_2F_5 \cdot 7H_2O$ exhibits a broad band due to the $Fe(H_2O)_6^{+2}$ ion with maxima at 9500 and 11200 cm^{-1}. The diffuse reflectance spectrum of the dihydrate exhibits a band of similar shape, but with maxima at 7900 and 9600 cm^{-1}. This red shift is consistent with coordination of Fe^{+2} by fluoride in $Fe_2F_5 \cdot 2H_2O$, since fluoride lies below water in the spectrochemical series. Apparently, as water, which is coordinated to Fe^{+2} in $Fe_2F_5 \cdot 7H_2O$, is lost upon dehydration the vacant coordination sites are filled by formation of fluoride bridge bonds.

Since iron (II) and iron (III) are linked by fluoride bridges in $Fe_2F_5 \cdot 2H_2O$, it is expected that there will be some interaction between them, e.g., that the material will be a Robin and Day Class II complex.[3] This expectation is verified by the diffuse reflectance spectra. In addition to the broad band near 9000 cm^{-1}, the spectrum of the dihydrate exhibits a maximum near 15000 cm^{-1}. This maximum is assignable to the intervalence transfer band, thus establishing that $Fe_2F_5 \cdot 2H_2O$ is a Class II mixed-valence material.

It should be emphasized here that the material which we have studied is not

identical to those previously described. In previous reports on the dihydrate
(or, as erronesously described in earlier reports, the trihydrate) the material
was prepared by the thermal dehydration of the heptahydrate.[2,8-11] We have, how-
ever, prepared the complex directly, bypassing the heptahydrate stage. This material
is analytically correct for $Fe_2F_5 \cdot 2H_2O$, and its room temperature Mössbauer spectrum,
magnetic susceptibility, and X-ray powder pattern appear to be comparable to those
of the dihydrate prepared by thermal dehydration of the heptahydrate. However, the
two forms of the dihydrate exhibit quite distinct thermal behavior.[15] Although it
is possible that the difference between these two forms can be ascribed totally to
a difference in crystallinity, it appears more probable (based on TGA, DTGA, DSC,
and kinetic parameters) that there is some more fundamental difference. We hope to
be able to comment more fully about any differences at a later date. It should be
emphasized that all measurements discussed here refer specifically to the crystall-
ine dihydrate prepared directly, rather than by dehydration.

Magnetic Susceptibilities

Figure 1 shows plots of magnetic susceptibility, reciprocal susceptibility, and
effective magnetic moment versus temperature for $Fe_2F_5 \cdot 2H_2O$ over the temperature
range 0-260K at a single applied magnetic field of 1.0 kG. The form of these curves
is not common for coordination complexes, and deserves comment. First, at higher
temperatures (ca 150-250 K) χ^{-1} appears to be approximately linear with temperature,
suggesting Curie-Weiss behavior. Furthermore, extrapolation of this linear portion
to $\chi^{-1} = 0$ leads to a large negative intercept, consistent with antiferromagnetic
ordering. In contrast to this, at temperatures lower than perhaps 150 K the curve
deviates markedly from linearity. As the temperature approaches 50 K there is a
rapid increase in susceptibility such that χ^{-1} falls, effectively to zero; which is
behavior typical of ferromagnetic ordering. However, the overall behavior is, in

fact, typical of ferrimagnetic ordering, with antiferromagnetic interactions lead-
ing to incomplete spin cancellation and a net ferromagnetic alignment. Since the
information attainable, and the treatment of the data, are different above and
below the ferrimagnetic Neel point, we will discuss the results for these two
regimes separately.

1. Magnetism above the Neel point.

Although the plot of reciprocal susceptibility versus temperature appears to
be linear above about 150K, more detailed examination indicates that there is in
fact still curvature. Thus, the least- squares fit to Curie-Weiss law behavior in
the temperature interval 150-200 K leads to an expression $\chi_m = \frac{5.65}{T+95}$, whereas the
expression calculated for the interval 200-250 K is $\chi_m = \frac{7.17}{T+174}$. Higher temperature
intervals lead to increasingly negative intercepts on the temperature axis, and it
may be concluded that the susceptibility only approaches Curie-Weiss law behavior
asymptotically at higher temperature.

Such behavior is, of course, expected on the basis of the molecular field
theory of ferrimagnetism.[16-18] Although more accurate and refined models, which
take specific cognizance of the fact that behavior is dependent on exchange inter-
actions, are available for the description of cooperative effects in antiferromag-
netic and ferromagnetic materials, molecular field theory provides at least quali-
tatively accurate descriptions for these materials, and for ferrimagnetically ordered
materials it is the only model which provides satisfactory agreement with experiment.
In the molecular field approximation the actual field acting on a particular atom
is assumed to be the sum of an applied magnetic field and the internal or "molecular"
field due to interactions with other atoms in the material. Thus, an iron (III)
atom is assumed to be subjected to an external field as well as a molecular field
resulting from its interaction (electrostatic, not magnetic, in origin) with both
its iron (II) and iron (III) neighbors. These assumptions lead to

the following form for the high temperature behavior of the susceptibility:

$$\frac{1}{\chi} = \frac{(T-T_c)(T-T_c')}{C(T-\theta')} \qquad (1)$$

where T_c, T_c', and θ' are functions of the various molecular field coefficients, which may be related to exchange integrals. This equation describes a hyperbola in which the susceptibility asymptotically approaches Curie-Weiss behavior at high temperatures, and becomes infinite at a characteristic temperature, the ferrimagnetic Neel point (T_c). Figure 2 shows the best fit of the experimental data (which is field independent) to this equation, and various parameters are indicated. The ferrimagnetic molecular field theory thus serves as a good model for the high-temperature magnetic behavior of $Fe_2F_5 \cdot 2H_2O$. Some deviation at low temperature is, of course, expected, since the susceptibility can never become infinite.

At high temperatures $(T \gg T_c)$ this equation reduces to the Curie-Weiss limit,

$$\frac{1}{\chi} = \frac{T-\theta}{C} \qquad (2)$$

where

$$\theta = T_c + T_c' - \theta' \qquad (3)$$

For $Fe_2F_5 \cdot 2H_2O$, the limiting high-temperature susceptibility is then given by

$$\chi = \frac{6.74}{T+179} \qquad (4)$$

The similarity of this expression to that obtained from a linear fit in the region 200-250 K suggests that above perhaps 250 K the complex has effectively attained its Curie-Weiss limit. The effective magnetic moment, calculated from $\mu_{eff} = 2.828\sqrt{C}$ is 7.34 B.M., and may be compared to a value of 7.91 B.M. predicted for <u>non-interacting</u> high-spin iron (II) and iron (III)[3], that is,

$$\mu_{eff} = [(\mu_{Fe}+2)^2 + (\mu_{Fe}+3)^2]^{\frac{1}{2}} \tag{5}$$

A related material, $LiFe_2F_6$, has been shown [19] to order antiferromagnetically at 105K, and for this species μ_{eff}, calculated in the same fashion, is 7.32 B.M. The negative value of θ in $\chi = \frac{C}{T-\theta}$ implies a negative exchange integral between Fe^{+2} and Fe^{+3}, e.g., antiferromagnetic interaction. This conclusion is consistent with the more quantitative results obtained from measurements of the saturation magnetization at low temperatures. The value of the ferrimagnetic Neel point, $T_c = 48$ K, is in excellent agreement with the value of $T_c = 48.6$ K obtained by Imbert, et.al.,[11] from low-temperature Mössbauer studies.

2. Low Temperature Magnetism

Below the ferrimagnetic Neel point (in this case, 48.0 K) long range order dominates the magnetic behavior of ferrimagnetic materials. Several features of the low-temperature magnetic properties of $Fe_2F_5 \cdot 2H_2O$ should thus be at least qualitatively predictable. These include: a) field dependent susceptibility; b) spontaneous magnetization; and c) a saturation magnetization at 0 K compatible with spin compensation of Fe^{+2} by Fe^{+3}. At any point in the temperature-field domain the observed magnetization is given by the difference between the individual sublattice magnetizations, e.g.,

$$M_{obs} = | M_{Fe}+3 - M_{Fe}+2 | . \tag{6}$$

In the absence of detailed knowledge of the individual sublattice magnetizations (which cannot be obtained from bulk magnetic measurements) it is impossible to quantitatively correlate experiment and theory, except at saturation. However, the observed magnetic properties of $Fe_2F_5 \cdot 2H_2O$ are in at least qualitative agreement with expectations, and our results are discussed briefly below.

a) Spontaneous magnetization.

Below the ferrimagnetic Neel point $Fe_2F_5 \cdot 2H_2O$ exhibits spontaneous magnetization in zero applied field. Figure 3 shows the variation of the reduced magnetization $(M(T)/M(0°K))$ as a function of the reduced temperature ($\tau = T/T_c$). The shape of the curve is at least qualitatively that of the Brillouin function, as expected. In the extreme case, where Fe^{+2} - Fe^{+2} and Fe^{+3} - Fe^{+3} interactions are negligible in comparison to Fe^{+2} - Fe^{+3} interactions, the curve should approximate the appropriate Brillouin function[20] with S = 1/2. This function, shown as the solid line in Figure 3, appears to provide a reasonable approximation to the data. Calculated curves with higher values of s provide a poorer fit to the experimental data. The observation that the curve with S = 1/2 provides a better fit is consistent with our interpretation that the ferrimagnetic behavior results from antiferromagnetic interactions between Fe^{+2} and Fe^{+3}. The shape of the magnetization curve approximates "Type Q" behavior,[16] which is the most commonly observed form for ferrimagnetic materials.

The Mössbauer work of Imbert, et.al.[11] demonstrates a clear discontinuity in the value of the magnetic hyperfine field at 26.5K. This discontinuity should be apparent in the magnetization curve as well, and may perhaps be reflected in the slight inflection in the curve near 25K. However, it is clear that the effect in the magnetization data is not nearly so significant as it is in the Mössbauer data, a difference which might be a result of our use of crystalline $Fe_2F_5 \cdot 2H_2O$, rather than the material prepared by thermal dehydration of the heptahydrate.

b) Field dependent susceptibilities.

As expected for a magnetically condensed system, the susceptibility becomes field dependent below the critical temperature, the susceptibility decreasing with increasing applied field. Although this field dependence is expected, the specific

behavior observed for $Fe_2F_5 \cdot 2H_2O$ is complicated, and suggests the existence of a distinct magnetic phase(s) which is as yet not characterized.

Figure 4 shows several sets of susceptibility versus temperature data in the range 0-75 K. The exact form of these data is dependent on the specifics of the measurements, and requires some comment. Curve A represents data obtained using the Faraday balance at an applied field of 2.23kG. It may be seen that the susceptibility exhibits a broad maximum near 20 K. Curve B represents data obtained using the vibrating sample magnetometer (VSM) at an applied field of 1000G. These measurements were obtained by first cooling the sample to helium temperatures in zero applied field, applying the 1000G field, and measuring susceptibilities while warming the sample. Although differing in detail, the forms of these curves are comparable, and once again the susceptibility maximizes at low temperature. Curve C, which again represents VSM data obtained at 1000G, differs from curve B in that the magnetic field was applied while the sample was being cooled. The data are identical when measured during either warm-up or cool-down operation. Significantly, there is no maximum in the susceptibility curve. Thus, there must exist some field dependent magnetic phenomenon which is effective at low temperatures, and which leads to the observed difference between susceptibilities obtained for samples cooled either in or out of the field. At fields above the apparent magnetic phase transition (vide infra) the susceptibility is independent of sample treatment. Thus, a sample cooled in zero applied field and measured at 15000G on the warm-up cycle provides a curve identical to that obtained upon cooling in the field. In this case, as for all experiments conducted after cooling in an applied field, no susceptibility maximum is observed.

c) Saturation magnetization

Figure 5 shows the variation in the magnetization, M, of $Fe_2F_5 \cdot 2H_2O$ (calculated as the product of the molar susceptibility and the applied field) as a function of

field at 4.2 K. As can be seen, the initial smooth increase in magnetization with increasing field is followed by an abrupt, and apparently discontinuous, increase at 14.7 kG. Following this rapid increase the magnetization is nearly constant with increasing fields up to 45 kG indicating that saturation has been reached. There is a marked hysteresis to this transition, since upon reducing the field the magnetization drops only slowly. The values of the magnetization at fields higher than the transition field, and at lower fields after first passing through the transition and then reducing the field, are comparable to values obtained upon cooling the sample in those applied fields, and of course much larger than the values observed following cooling in zero applied field and then raising the field to the appropriate value. Although a detailed interpretation of these observations has not proven possible, e.g., some type of spin-flop, meta-magnetic or canting behavior, this behavior is in at least qualitative agreement with the field dependent behavior discussed above. As expected from the field dependent behavior, the values of the magnetization below the transition field depend upon the sample's magnetic history but are independent of it above the transition. Unexpectedly, however, both the field at which the transition occurs and also the magnitude of the discontinuity appear to depend upon sample history, the rapid increase occurring on different occasions within the interval 11 to 15 kG. In fact, there may be several transitions involved at ca 15 kG which are not readily resolved in powder magnetization studies.

The saturation magnetization, M, at 0 K may be related to a saturation moment, μ_{sat} by

$$\mu_{sat} = \frac{M}{N\beta} \qquad (7)$$

Since saturation appears to be obtained at fields above the transition, and since this saturation moment is nearly independent of temperature below about 4 K, the magnetization at 1.75 K and 15 kG may be taken as a good approximation to the zero degree saturation magnetization. The observed value is $\mu_{sat} \cong 1.2$ B.M. Since the

saturation moment is the maximum component of the magnetic moment in the direction of the applied field, e.g.,

$$\mu_{sat} = g\beta S, \qquad\qquad (8)$$

it is possible to relate the spin and magnetization. A positive exchange interaction between Fe^{+2} and Fe^{+3} (e.g., ferromagnetism) would lead to a "molecular" spin of $S = 9/2$, hence a value of $\mu_{sat} = 9$ B.M., assuming the free-electron g-value of 2.0. By contrast, a negative exchange interaction between Fe^{+2} and Fe^{+3} (e.g., the ferrimagnetic behavior as claimed here) leads to a molecular spin $S = 1/2$, hence an expected value of $\mu_{sat} = 1.0$ B.M. This is in excellent accord with the experimental value $\mu_s = 1.2$ B.M. This provides strong evidence for the existence of ferrimagnetic ordering in $Fe_2F_5 \cdot 2H_2O$.

Mössbauer Spectra

Conformation of pentafluoro-diiron (II,III) - dihydrate as a Class II rather than a Class III substance[3] is provided unambiguously by the Mössbauer spectra obtained above 50 K. The spectrum at 295 K (Figure 6) shows three distinct lines. The only reasonable assignment of Mössbauer parameters requires the assumption of overlapping Fe(II) and Fe(III) components of separate quadrupole split doublets. According to this view[10,11,21] two distinct quadrupole-split doublets exist, with parameters which are indicative of "trapped" valences -- i.e., distinguishable Fe(II) and Fe(III) sites on the Mössbauer time-scale. The best supporting evidence for the peak assignments is the spectrum obtained at 57°K (Figure 7) which clearly shows all four lines. The isomer shifts and quadrupole splittings of both Fe(II) and Fe(III) sites are similar to reported values for iron fluoride compounds[22] and, in particular, to the mixed-valence salt $LiFe_2F_6$[23] (Table I).

Substance	δ_{+2}	Δ_{+2}	δ_{+3}	Δ_{+3}	Temp(K)	Ref
$Fe_2F_5\cdot2H_2O$	1.58	2.57	0.73	0.56	293	10
$Fe_2F_5\cdot2H_2O$	1.59	2.50	0.73	0.59	295	11
$Fe_2F_5\cdot2H_2O$	1.60	2.44	0.70	0.65	295	this work
$LiFe_2F_6$	1.61	2.53	0.72	0.45	295	23
$Fe_2F_5\cdot2H_2O$	1.71	3.31	0.86	0.59	80	10
$Fe_2F_5\cdot2H_2O$	1.73	3.30	0.78	0.58	50	11
$Fe_2F_5\cdot2H_2O$	1.71	3.28	0.81	0.58	55	this work
$LiFe_2F_6$	1.76	3.10	0.83	0.40	78	23

Table I. Reported Mössbauer parameters for $Fe_2F_5\cdot2H_2O$ and $LiFe_2F_6$. All values for isomer shifts (δ) and quadrupole splittings (Δ) are in mm/sec, and isomer shifts are corrected relative to a sodium nitroprusside standard.

For the iron (III) sites, with $Fe^{III}F_6$ coordination, the room temperature isomer shift (0.70 mm/sec) is close to that of K_3FeF_6(.68 mm/sec). The iron (III) quadrupole splitting (0.65 mm/sec) is surprisingly large for a material only slightly distorted from octahedral symmetry, and is, in fact, larger than in the $[FeF_5(H_2O)]^{2-}$ ion.[5] Although no other ion with the trans-$Fe^{II}F_4(H_2O)_2$ configuration is known, the isomer shift (1.60 mm/sec) observed for iron (II) in $Fe_2F_5 \cdot 2H_2O$ is comparable to values in other ionic fluorides, and the quadrupole splitting (2.44 mm/sec) is close to the values observed in $FeCl_2 \cdot 2H_2O$ and $FeBr_2 \cdot 2H_2O$ (2.50,2.49 mm/sec), both of which have the trans - $FeX_4(H_2O)_2$ structure. Although there does appear to be general agreement between our findings and previous reports[10,11,21] of high temperature Mössbauer studies of the iron fluoride dihydrate, a closer examination of the tabulated results reveals a significant variation in certain of the parameters, particularly at room temperature. In all of the published spectra, as well as in our own work, the room temperature Mössbauer spectrum consists of three lines. The more intense peak at low velocity is assumed to result from an accidental degeneracy (in velocity) of the low-velocity branches of quadrupole split Fe^{+2} and Fe^{+3} spectra. This degeneracy must be nearly exact, since the absorption exhibits no broadening, and since attempts to fit this peak as the superimposition of two peaks lead to no significant improvement in the fit, and to identical velocities for both components. Under these conditions, that some peak velocity is used in the calculation of isomer shifts and quadrupole splittings for both Fe^{+2} and Fe^{+3}. Conversely, that peak position should be calculable from reported isomer shifts and quadrupole splittings according to:

$$\text{velocity} = \delta_{+n} - \frac{\Delta_{+n}}{2} , \qquad (9)$$

and should yield identical values of the peak velocity for both n = 2 and n = 3. However, examination of the data from references 10 and 11 shows that the

peak positions calculated from the Fe^{+2} and Fe^{+3} parameters differ by 0.14 and 0.10 mm/sec, respectively. Consequently, either these authors were able to resolve the individual components of this absorption - a resolution which appears incompatible with published information - or else the calculations are in error. We suspect that this is the case, and is the factor most likely to account for the discrepancy between published values and our work.

Some of the differences in reported parameters may also arise in the modes of preparation. We have employed a novel preparation of the dihydrate which appears to give a highly stable, reproducible product which analyzes correctly as $Fe_2F_5 \cdot 2H_2O$. All preparations of $Fe_2F_5 \cdot 2H_2O$ reported previously have followed a method suggested by Brauer[2]; i.e., thermal dehyration of $Fe_2F_5 \cdot 7H_2O$ at 100°C. Although Sakai and Tominaga[21] have published thermogravimetric data which support the observation of a smooth, continuous dehydration from heptahydrate to dihydrate, we believe that the process is, in fact, complex[15] and that care must be taken in the preparation so as to avoid loss of HF and a consequent F-deficiency in the product.[24] It is quite possible that the compositional integrity of $Fe_2F_5 \cdot 2H_2O$ may be dependent upon its mode of preparation. Although this is as yet unproved, it seems proper to enlist care in the comparison and interpretation of results from various laboratories.

The Mössbauer spectra of $Fe_2F_5 \cdot 2H_2O$ at 20 K, $H_o=0$ and at 4.2K, $H_o=0$, and longitudinal fields of 5 and 60 kG are shown in Figures 8 and 9 respectively. The ferrimagnetic ordering of the material is reflected in the hyperfine splitting at 20K where two subspectra (Fe^{+2} and Fe^{3+}) are apparent and labeled with stick diagrams. The primed transitions correspond to the ferric sublattice and the double prime to the ferrous. The transitions of the ferric sublattice are sufficiently resolved so that one may obtain accurate values of the effective hyperfine field (H_n) at the Fe^{3+} sites. As a starting approximation, since the quadrupole interaction at the ferric sites is

considerably smaller than the Zeeman splitting, one can estimate H_n from the overall spectral splitting. In this case $\Delta_{1'-6'} = 14.67$ mm/sec from the least squares fit implying $H_{eff} = 454$ kG. More accurate values for H_n can be obtained from the $I = 1/2$ ground state Zeeman splitting (there is no quadrupole splitting for the ground state) as deduced from the separation of transition pairs terminating in the same m_I sublevel of the $I = 3/2$ excited state. The spectral pairs involved are 3' and 5' and 2' and 4' for which least squares fitting gives $\Delta_{3'-5'}$ and $\Delta_{2'-4'}$ equal to 5.44 and 5.51 mm/sec respectively corresponding to $H_n = 457$ kG and 463 kG for a ground state splitting of 0.1188 mm/sec/Tesla or thus an average value of Hn = 460 kG at Ferric sites at 20 K. An easy check on our choice of appropriate pairs comes from the fact that the area of such pairs should equal[25] one-fourth of the total spectral absorption intensity for a thin absorber. For the least squares fit of Figure 8 and the pairs we have chosen, this is precisely the case. Imbert, et.al.[11] have examined the Mössbauer spectra of this material in detail. From their analysis of the Fe(II) sub-spectrum, they concluded that Fe(II) ions existed in an axial crystal field, in agreement with the structural results, and that Fe(II) exhibit a strong magnetic anisotropy, again consisted with expectations based on the structure.

The Mössbauer spectrum of $Fe_2F_5 \cdot 2H_2O$ at 4.2K, H = 0, is very similar to that at 20K except that the effective field at the ferric sites has increased, i.e., $H_n = 532$ kG. This result agrees favorably with that of Imbert, et.al., who found $H_n = 538$ kG. Based on that value and a comparison to iron fluorides of known structure, they concluded that the geometry at Fe(III) was $Fe^{III}F_5(H_2O)$, as in the complex $Fe_2F_5 \cdot 7H_2O$. However, the crystal structure of $Fe_2F_5 \cdot 2H_2O$ clearly demonstrates $Fe^{III}F_6$ coordination.[12]

Spectra in small and large applied fields show degrees of broadening and no obvious evidence of field induced phase transitions such as are observed from susceptibility measurements. Some interesting observations can be made from the field

dependence of the powder spectra. First of all, one sees a positive hyperfine field at the ferric sites. That is at 4.2 K the value of H_n at the ferric sites is 549 kG for H_o = 60 kG or an increase of $\sim$ 17 kG relative to H_o = 0. A comparable effect is observed for $FeF_3 \cdot 3H_2O$ for which H_n increases from 446 to 456 kG on increasing the applied field from 0 to 60 kG. In Figure 9 it should also be noted that transitions 2' and 5' (the Δm_I = 0 transitions) of the ferric subspectrum have intensified relative to 1' and 6' indicating rotation of the spin moments of the crystallites and thus their magnetization to a direction normal to that of the applied field. Powder samples of $FeF_3 \cdot 3H_2O$ also show a similar field dependent behavior. For sufficiently large applied fields, it is possible for canting of the Fe^{2+} and Fe^{3+} sublattice moments to occur. However, the high critical temperature of the present system and concomittant strong intersublattice exchange interaction suggests that such canting will be negligible and not observable in the powder Mössbauer spectra.

To conclude it is worthwhile to compare some of our low temperature results with those for the higher hydrate $Fe_2F_5 \cdot 7H_2O$. This material orders at T < 3 K and the details of its zero field Mössbauer spectrum at 1.3 K have been discussed.[26] In contrast to the dihydrate there appear to be two slightly different but near equally populated ferric sites for which H_n = 561 and 573 kG. The effective field at the ferrous sites of $Fe_2F_5 \cdot 7H_2O$ is 146 kG at 1.3 K and is much larger than that observed (41 kG) for the ferrous sites of the dihydrate. The considerable difference in the critical temperatures of these materials, 48.0 K for the di-hydrate versus < 3 K for the heptahydrate, suggests that the former must be magnetically more condensed owing to extensive bridging. This is consistent with the proposed discrete ion, $[Fe(H_2O)_6^{2+}][Fe\ F_5(H_2O)^{2-}]$ structure of the hepta-hydrate.
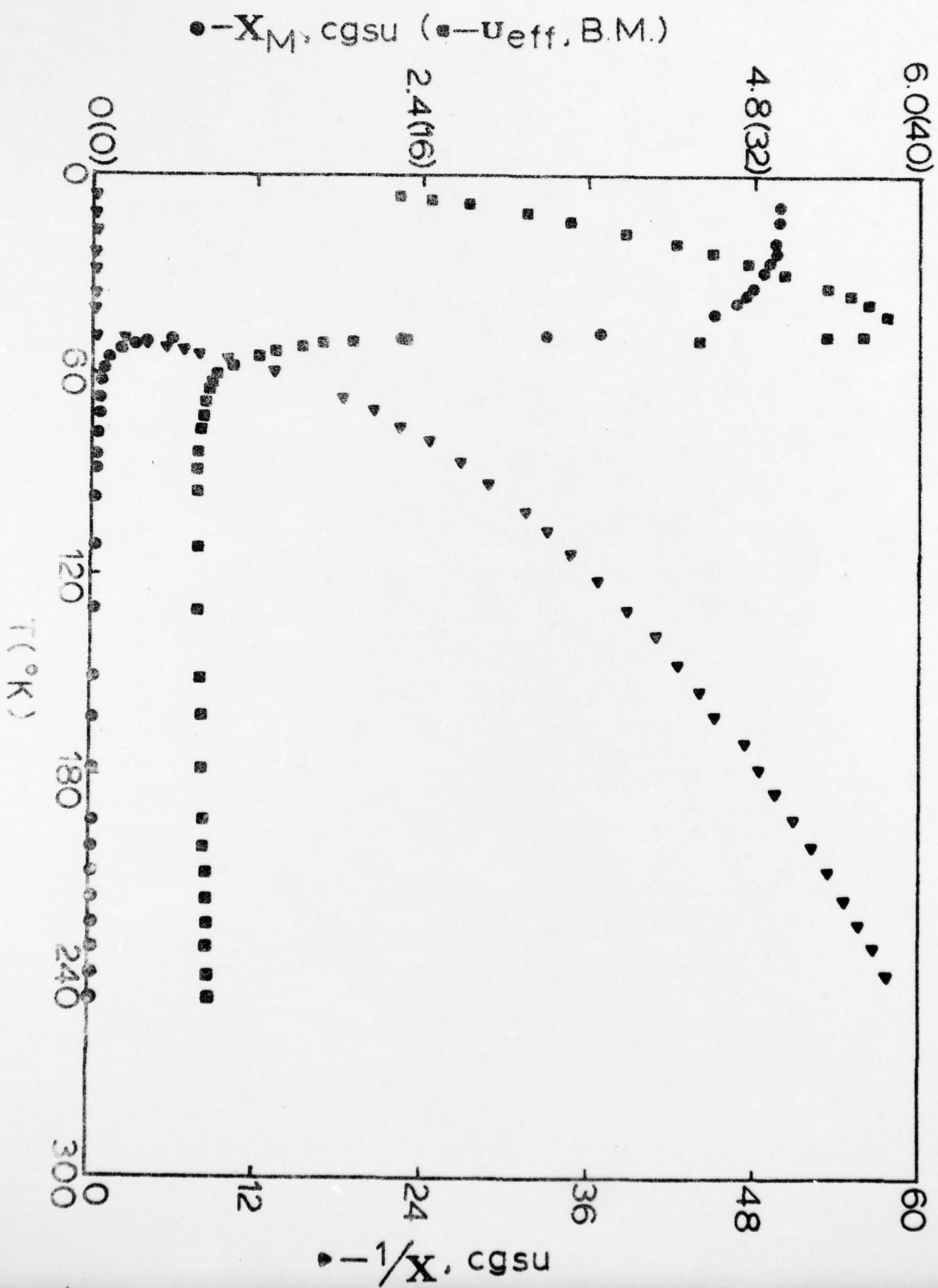
Acknowledgements
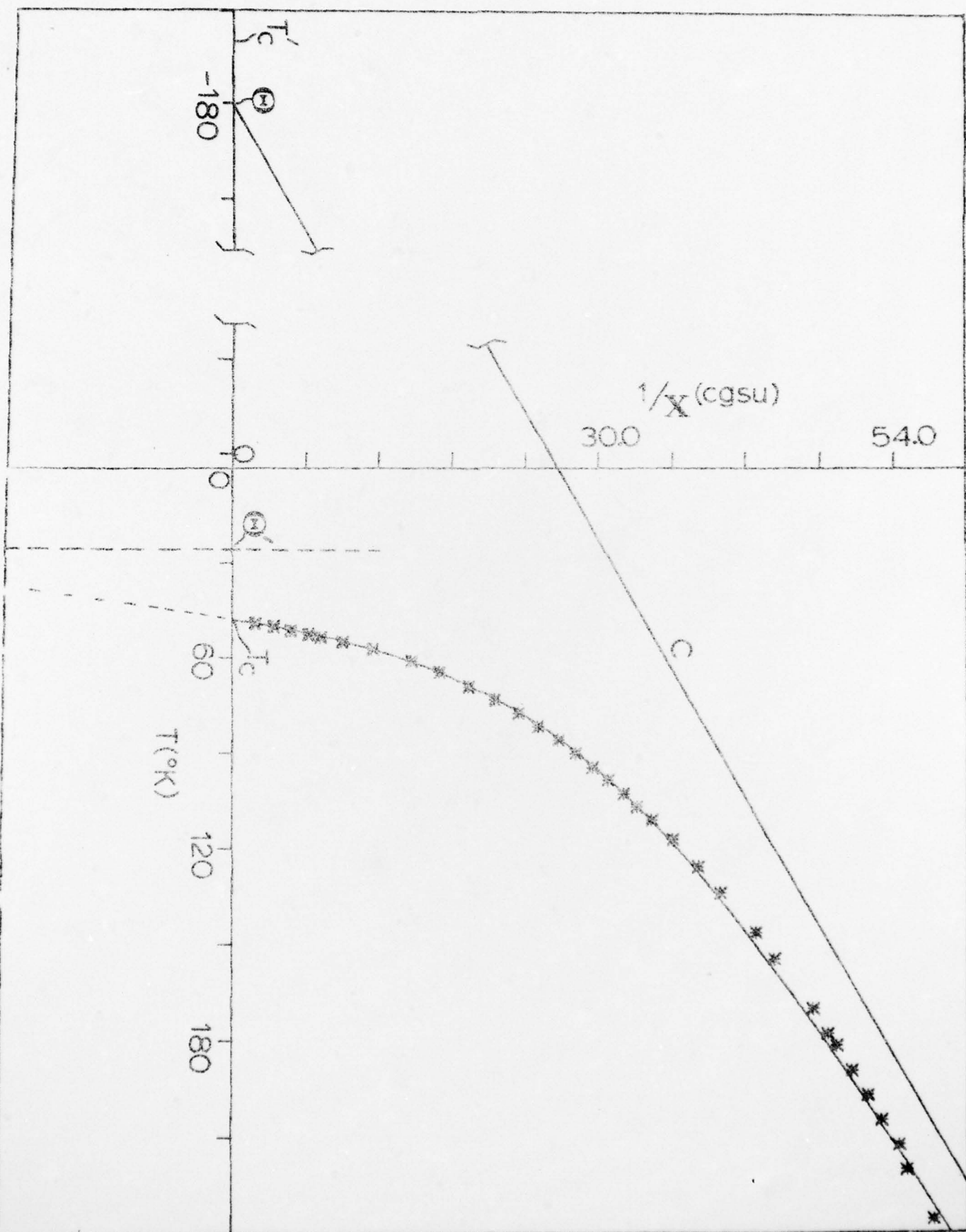
References and Notes

1. (a) University of Vermont. Hood Interdisciplinary Fellowship Awardee.
   (b) University of Vermont.
   (c) Northeastern University.

2. G. Brauer and M. Eichner, Z. Anorg. Allg. Chem. 296, 13 (1958).

3. M.B. Robin and P. Day, Adv. Inorg. and Radiochem. 10, 247 (1967).

4. J. Portier, Angew. Chem. Intl. Edit. Engl., 15, 475 (1976).

5. E.G. Walton, P.J. Corvan, D.B. Brown, and P. Day, Inorg. Chem., 15, 1737 (1976).

6. T. Sakai and T. Tominaga, Bull. Chem. Soc. Jap. 48, 3168 (1975).

7. D.B. Brown and E.G. Walton, Abstracts of Papers, 170th National Meeting of the
   American Chemical Society, Chicago, August 1975.

8. P. Charpin and Y. Machetau, Compte. Rend. C280, 61 (1975).

9. K.J. Gallagher and M.R. Ottaway, J.C.S. Dalt. Trans., 987 (1975).

10. T. Sakai and T. Tominaga, Radioisotopes 23, 347 (1974).

11. P. Imbert, G. Jehanns, Y. Macheteau, and F. Varret, J. Physique 37, 969 (1976).

12. W. Hall, S. Kim, J. Zubieta, E.G. Walton, and D.B. Brown, Inorg. Chem. 16, 0000
    (1977).

13. B.N. Figgis and R.S. Nyholm, J. Chem. Soc. 4190 (1958).

14. Reference 5, Figure 2.

15. J.A. Dilts, E.G. Walton, and D.B. Brown, unpublished observations.

16. J.S. Smart, "Molecular Field Theories of Magnetism," W.B. Saunders, Phila. (1966).

17. J.S. Smart, Am. J. Phys. 23, 356 (1955).

18. J.B. Goodenough, "Magnetism and the Chemical Bond", Wiley/Interscience, New York (1963).

19. J. Portier, A. Tressand, R. De Pape, and P. Hagenmuller, P.C.R. Hebd. Seances Acad.
    Sci, Ser. C., 267, 1711 (1968).

20. Ref. 16, Equation 3.19.

21. T. Sakai, and T. Tominaga, Radiochem. Radioanal. Letters, 23, 329 (1975).

22. N.N. Greenwood, and T.C. Gibb, Mössbauer Spectroscopy, Chapman & Hall, 1971.

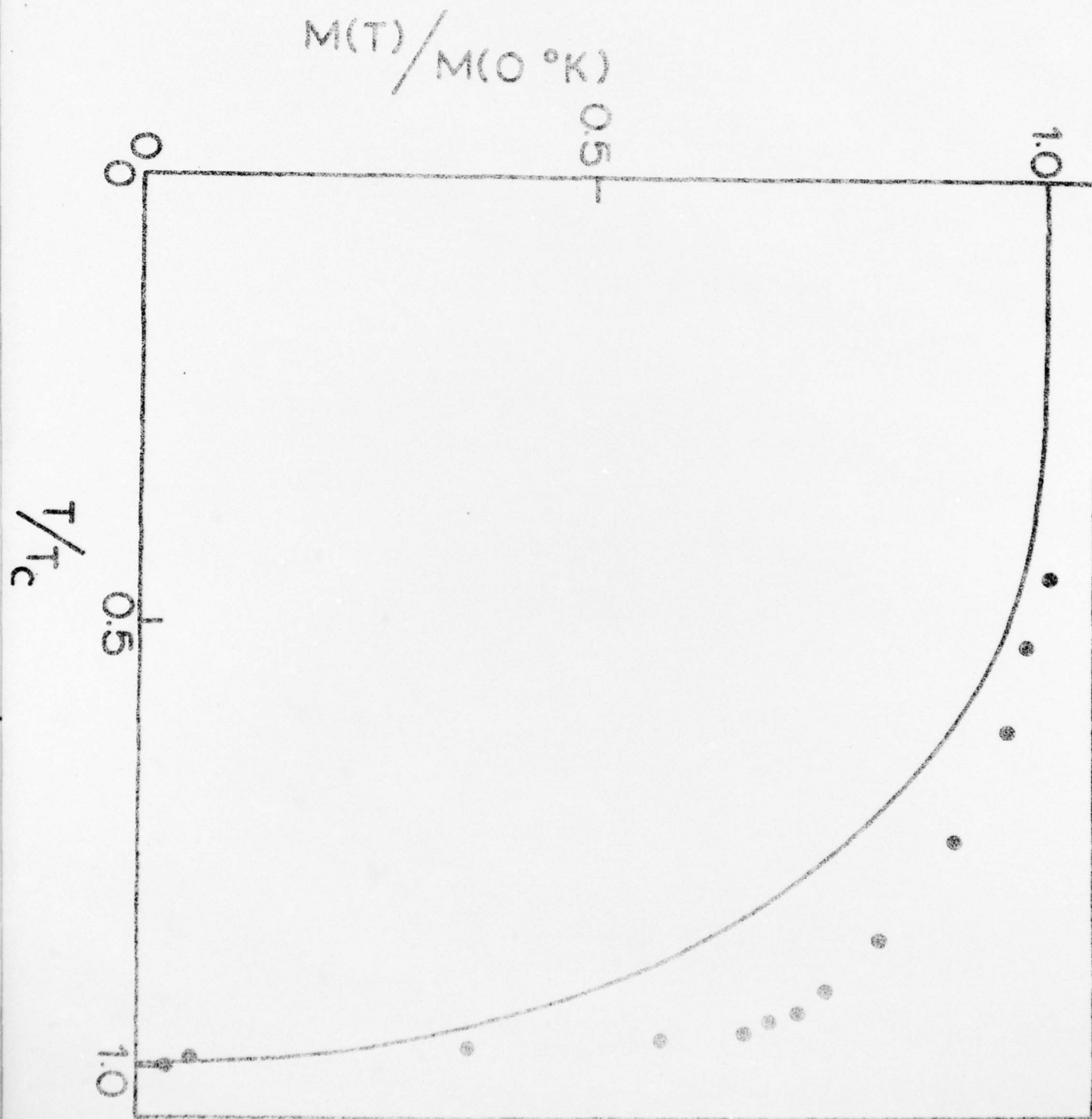23. N.N. Greenwood, A.T. Howe, and F. Memil, J. Chem. Soc. (A), 2218 (1971).

22

24. Sakai and Tominaga (Ref. 10) have produced analyses of $Fe_2F_5 \cdot 2H_2O$ which exhibit a F/Fe ratio of 4.8/2.

25. J. Van Dongen Torman, R. Jagannathan and J.M. Trooster, Hyperfine Interactions $\underline{1}$, 135 (1975).

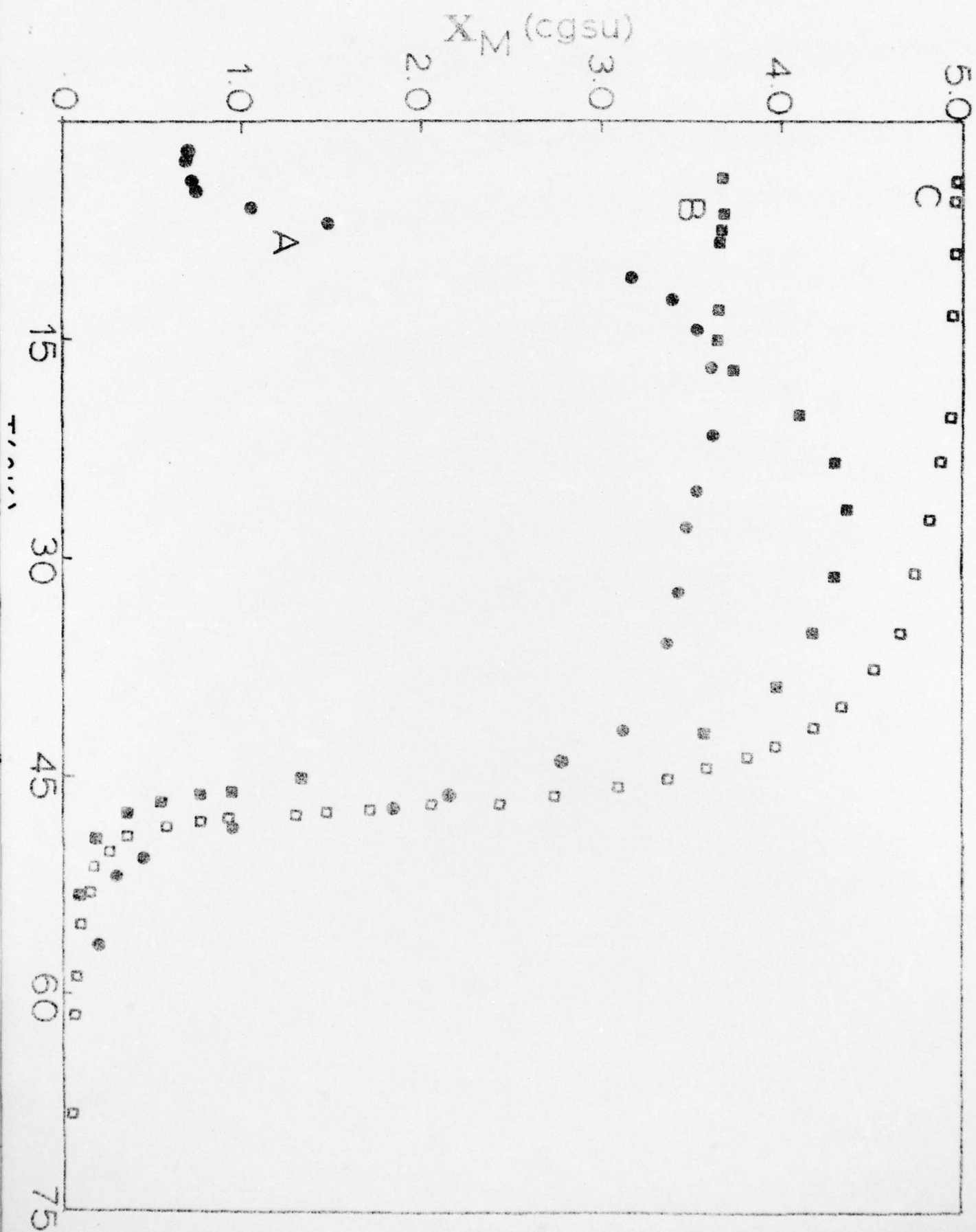26. P. Imbert, Y. Macheteau and F. Varret, J. Phys. (Paris) $\underline{34}$, 49 (1973).

Figure Captions

Figure 1. Molar susceptibility (◉), inverse susceptibility (▼), and effective magnetic moment (■) for $Fe_2F_5 \cdot 2H_2O$ as a function of temperature. Data obtained at an applied field $H = 1000$ kG, with the sample cooled in the field.

Figure 2. Reciprocal susceptibility (✳) versus temperature above the Neel point. The solid line is the best fit of equation (1) to the experimental data, with $T_c = 48.0$, $T_c' = -200.9$, $\theta' = 25.8$, and $C = 6.74$. The solid line represents the Curie-Weiss limit, calculated from equations (2)-(4).

Figure 3. Spontaneous magnetization of $Fe_2F_5 \cdot 2H_2O$, plotted as reduced magnetization (◉) versus reduced temperature, assuming $T_c = 48.5$ K. The solid line is the Brillouin function for $S = 1/2$.

Figure 4. Susceptibility versus temperature below the Neel Point. Curve A(◉) - Faraday balance data, 2.23 kG. Curve B (■) - VSM data, 1.0 kG. Data obtained following cooling in zero applied field. Curve C (□) - VSM data, 1.0 kG. Data obtained following cooling in 1.0 kG applied field.

Figure 5. Magnetization at 4.2 K as a function of increasing magnetic field, following cooling in zero applied field.

Figure 6. Room temperature Mössbauer spectrum of $Fe_2F_5 \cdot 2H_2O$. The solid lines through the data points represents a best fit to the sum of the three lorentzian peaks indicated.

Figure 7. Mössbauer spectrum of $Fe_2F_5 \cdot 2H_2O$ at 55 K. The solid line through the data points represents a best fit to the sum of the four lorentzian peaks indicated.

Figure 8. Mössbauer spectrum of $Fe_2F_5 \cdot 2H_2O$ at 20 K. The solid line through the data points represents a best fit to the sum of eleven lorentzian lines. Individual Fe^{+2} and Fe^{+3} subspectra are labeled with stick diagrams.

Figure 9. Mössbauer spectra of $Fe_2F_5 \cdot 2H_2O$ at 4.2 K in longitudinal applied fields of 0, 5, and 60 kilogauss.
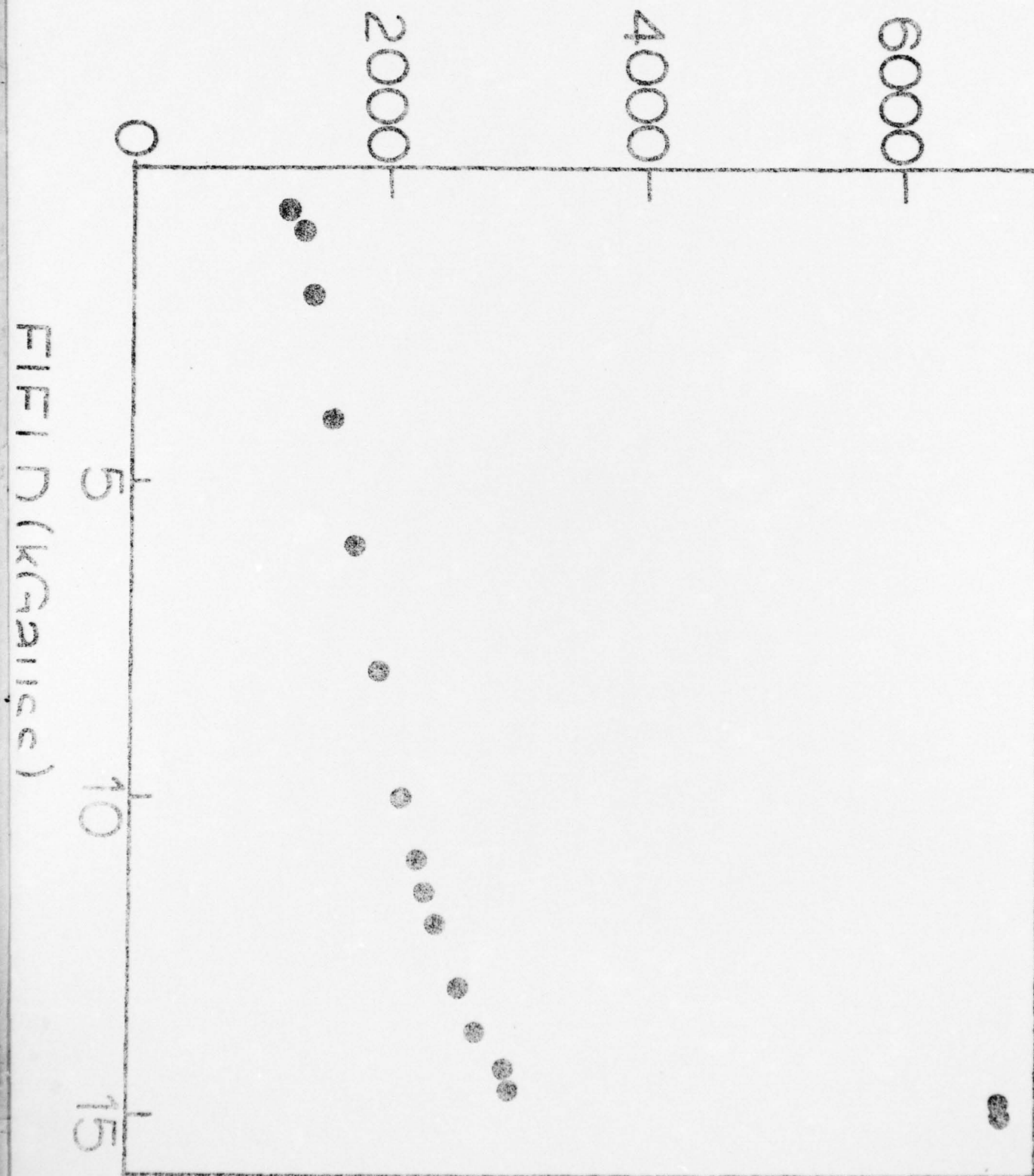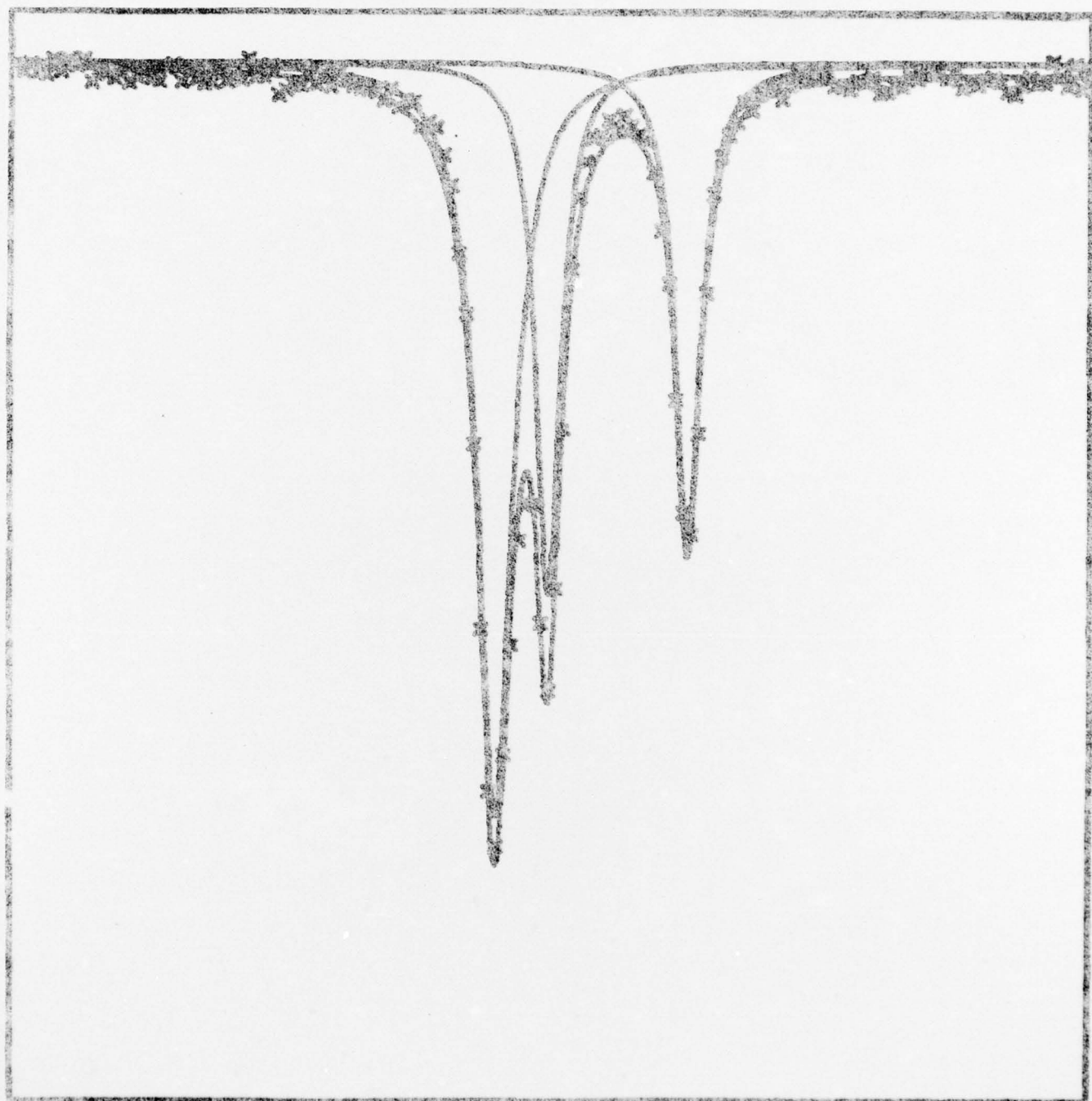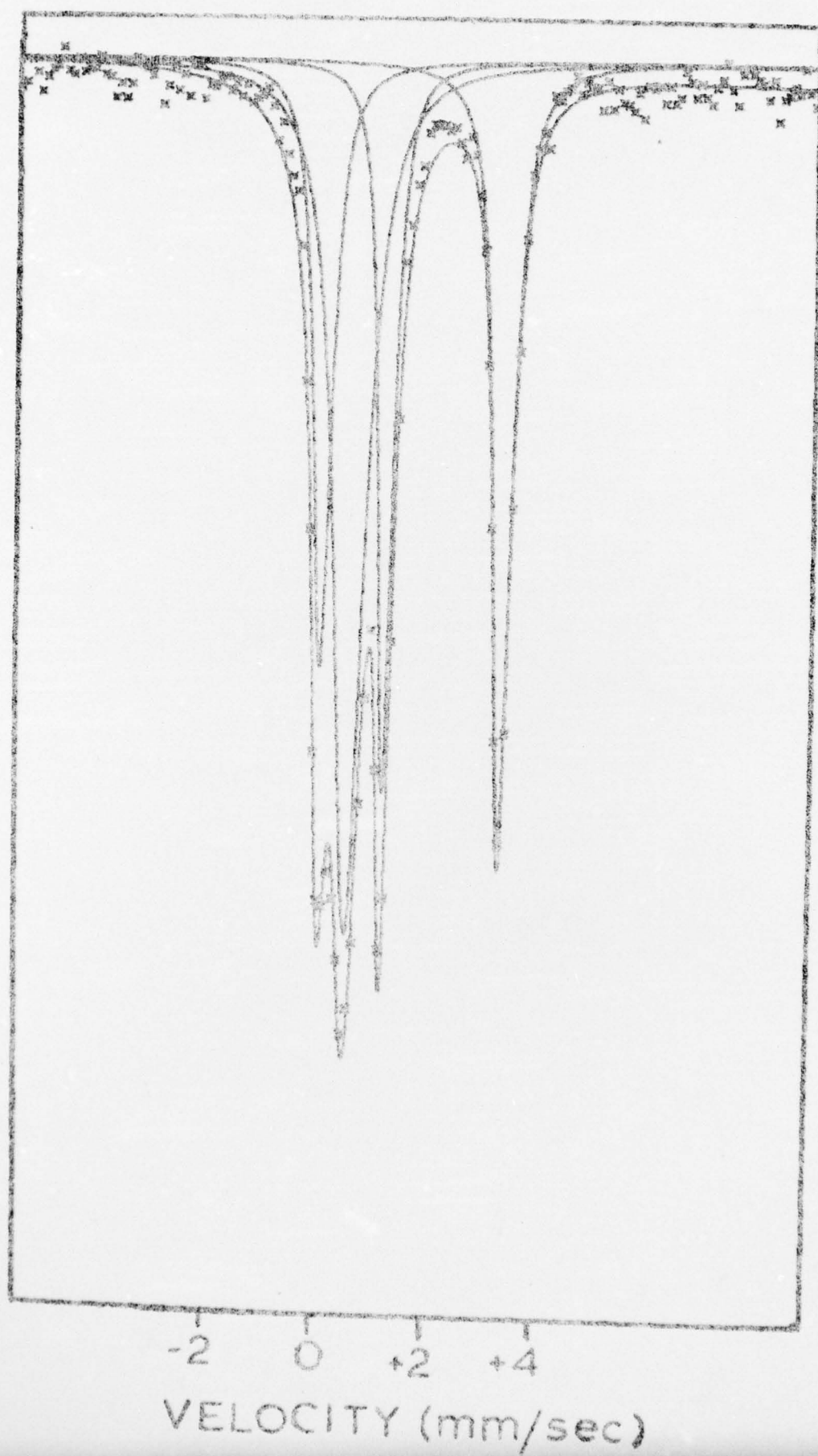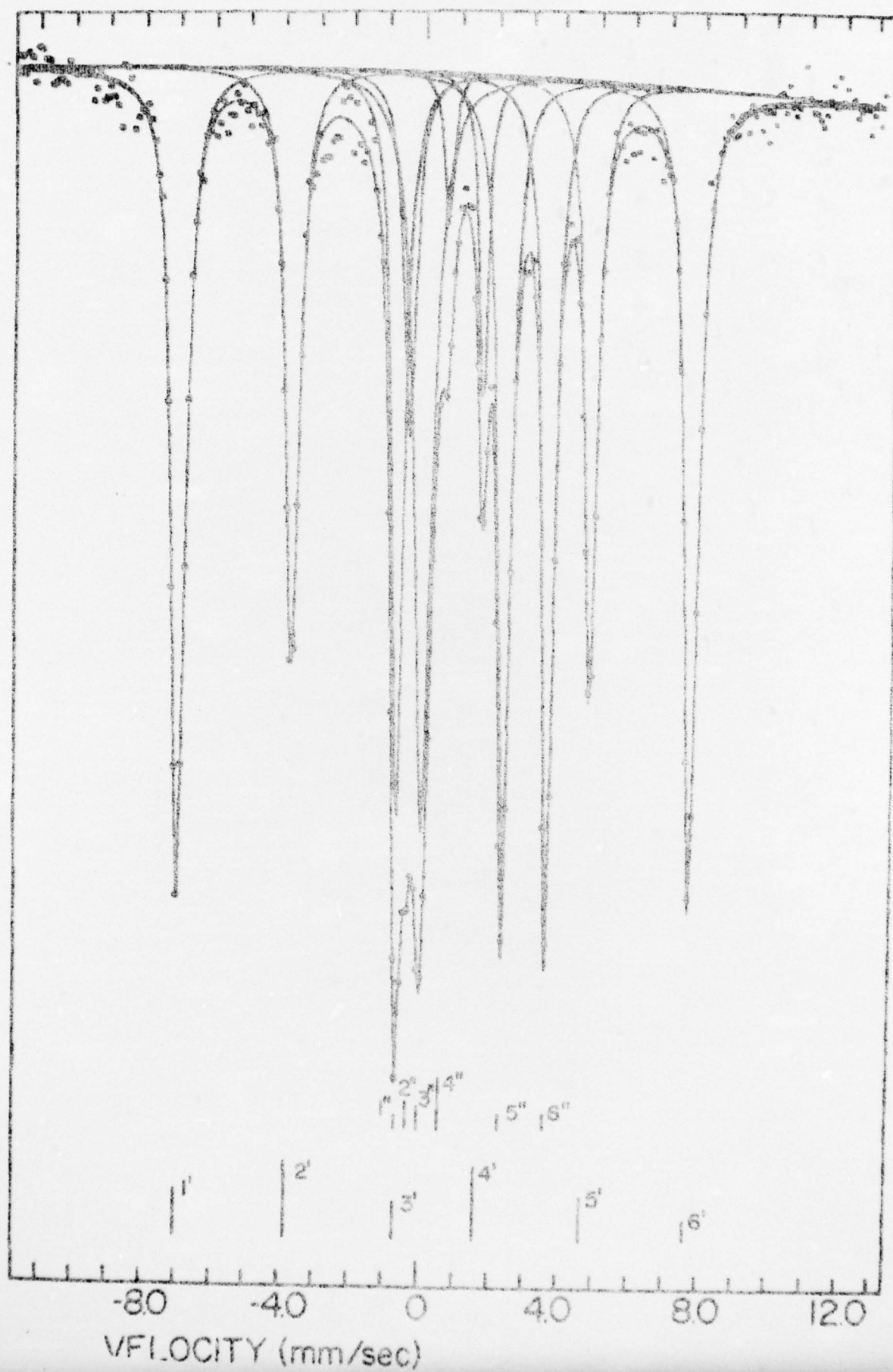
$1/\chi$ (cgsu)

T_c

-180

30.0

54.0

0

T_c

60

120

180

T(°K)

C

M(T)/M(O °K)

0

0.5

1.0

T/T$_c$

0.5

1.0

VELOCITY (mm/sec)